Geochemistry, Rb-Sr whole rock age and Sr-Nd isotopic constraints on the Variscan A₁-type granite from Azegour area in the Marrakech High Atlas (Moroccan Meseta) and their geodynamic implications

Mohamed Hadani[1]*, Maria do Rosário Azevedo[2], Rui Dias[3], Adil Saeed[4], Salah F. Awadelsied[4]

[1]Geodynamic and Geomatic Labrotory, Department of Geology. Chouaib Doukkali University, Route Ben Maachou, B.P.20, 24.000 El Jadida, Morocco
[2]Department of Geosciences, University of Aveiro, Campus de Santiago, 3810-193 Aveiro, Portugal
[3]Institute of Earth Sciences, Department of Geosciences, School of Science and Technology of the University of Evora, 7000-671 Evora, Portugal
[4]Department of Mineral Resources, College of Petroleum Geology and Minerals, Bahri University, Khartoum 1660, Sudan
*corresponding author, e-mail address: geohadani@hotmail.com

Abstract

In the northern part of the Marrakech High Atlas (MHA), along the southern Variscan segment of the Western Meseta, a Variscan granitic intrusion crops out, intruding metasediments and meta-volcanosedimentary rocks of Early Cambrian to Ordovician age. A new whole-rock Rb-Sr isochron age of 268 ± 9 Ma for the granite, combined with a previously published whole-rock Rb-Sr radiometric dating (271 ± 3 Ma), reveals a post-kinematic (tectonic) character with regard to the main Variscan deformational event, belonging within the tectonic context of the Moroccan Variscan orogenic belt. Geochemically, the Azegour intrusion is metaluminous to peraluminous and exhibits a calc-alkaline affinity with a ferruginous composition. The massif shows an extremely differentiated character (SiO_2 = 77.53–78.14 per cent), K_2O and high total alkali contents, $FeO_t/(FeO_t + MgO)$ and Ga/Al ratios, which have typical characteristics of an A-type granite. In addition, the granite contains high concentrations of LREE (La_N/Sm_N = 7.9–13.67) relative to HREE (La_N/Yb_N = 4.81–11.61) and a well-defined Eu negative anomaly (Eu/Eu* = 0.44–0.75). The granitic samples exhibit a strong enrichment of the most incompatible elements (Rb_N/Yb_N = 69.84–159.98) and a strong depletion of Ba, Sr, Eu, Nb, P and Ti. These characteristics are similar to those of A₁-type granites. The absence of mineralogy typical of an S-type granite, combined with its weakly peraluminous character [A/CNK (molar $Al_2O_3/CaO+Na_2O+K_2O$) = 1,013–1,045], suggest that there is little or no significant involvement of supracrustal sources in the petrogenesis of the intrusion studied. Despite the strongly differentiated character of Azegour granitic rocks samples, their multi-element patterns shows many similarities to those of I-type granitoids, which has led to postulate that the parental liquids of A₁-type were derived from partial melting of mafic magmas. The representative samples studied show less depleted $\varepsilon Nd_{(t = 270\ Ma)}$ values of –0.94 to –4.85 and lower positive to slightly negative $\varepsilon Sr_{(t = 270\ Ma)}$ values of –1.45 to 9.32. The isotopic data suggest that the Azegour granite was emplaced 270 myr ago, apparently generated by partial melting of a mafic/intermediate magma source in the lower crust as a result of the underplating of the asthenosphere mantle-derived Oceanic Island Basalt-like magmas. Alternatively, their isotopic signatures also can be attributed to the interaction and/or hybridisation of basaltic liquids derived from the mantle with these lower crust materials. The generated parental magma probably occurred at deep structural levels and involved fractional crystallisation processes by the separation of a mineralogical association composed of plagioclase + potassium feldspar ± biotite ± amphibole ± sphene ± apatite. The whole-rock Rb-Sr age of 268 ± 9 Ma, whole-rock geochemistry and Sr-Nd isotopic compositions of $\varepsilon Nd_{(t = 270\ Ma)}$ and $\varepsilon Sr_{(t = 270\ Ma)}$, combined with fieldwork data, suggest that the Azegour granite was emplaced during the later stage of compressional Variscan events in the MHA.

Keywords: Rb-Sr whole-rock geochronology, whole-rock geochemistry, post-collisional processes, magma underplating, Variscan orogeny, Morocco

1. Introduction

Granitoids are major components of the continental crust. Their study has led to understanding the conditions of emplacement of intrusion rocks in their deformed Variscan basement (e.g., Lagarde & Choukroune, 1982; Vigneresse, 1995; Essaifi et al., 2001; Lécuyer et al., 2017; Delchini et al., 2018; Chopin et al., 2023). Although the generation of granitic magmas can take place in almost all geotectonic environments (e.g., White & Chappell, 1983; Pearce et al., 1984; Whalen, 1985; Maniar & Piccoli, 1989; Eby, 1992; Moyen et al., 2017; Castro, 2021), the intrusion of large volumes of granitic rocks is preferably associated with areas where the continental crust had been thickened as a consequence of collisional mountain building, such as ocean-continent or continent-continent convergence. Indeed, during the collisional and post-collisional phases of the Variscan orogeny, the meta-igneous and/or metasedimentary rocks of the (upper or lower) continental crust may have easily reached partial melting conditions and produced significant amounts of voluminous granitic magmas (e.g., Barbarin, 1999; Bonin, 2007; Castro, 2014; Moyen et al., 2017; Liu et al., 2020). However, the direct or indirect contribution of the mantle to these processes should not be underestimated. The heat required to melt the crust is provided by the rise of basaltic magmas derived from the mantle. These magmas can still interact, to varying degrees, with the residual and/or crustal rocks materials to form liquids with mixed signatures (e.g., Pitcher, 1983; White & Chappell, 1983; Brown et al., 1984; Pearce et al., 1984; Whalen, 1985; Cui et al., 2021).

In the classification scheme proposed by Chappell & White (1974, 1992) granites are linked to source rock compositions. I-type granites are primarily metaluminous and typically derived from meta-igneous source rocks, whereas S-type granites are strongly peraluminous and produced by partial melting of metasedimentary source material. Granitoid rocks may be divided into those generated during the evolution of fold-thrust belts (orogenic) and those associated with uplift and major strike-slip faulting (anorogenic) (Whalen et al., 1987). Anorogenic or A-type granites, initially defined by Loiselle & Wones (1979) and further discussed by Collins et al. (1982), Collerson (1982), Whalen & Currie (1984) and Whalen (1986), have recently received significant interest, essentially due to their economic potential and tectonic setting (e.g., Bonin, 2007; Grebennikov, 2014; Li et al., 2014; Vonopartis et al., 2021).

There is a wide variety of rocks that fall into the A-type classification, making it possible to classify them into two main categories (Eby, 1990, 1992):

a) A_1-type granitoids, generally referred to as anorogenous granites, which assume an origin from the differentiation of Oceanic Island Basaltic (O.I.B) magmas from enriched mantle sources, contaminated to varying degrees by crustal materials.

b) A_2-type granitoids, normally associated with post-collisional or post-orogenic geodynamic environments. The genesis of these granitoids may be related to either the interaction of mantellic magma with crustal rocks or with the partial fusion of exclusively crustal sources.

The present-day structure of the Moroccan Variscan belt is mainly the result of oblique convergence between the Gondwana and the Laurasia supercontinents during the late Palaeozoic (e.g., Ribeiro et al., 1979; Matte, 2001; Michard et al., 2010; Martínez-Catalán et al., 2021; Arenas et al., 2021; Chopin et al., 2023). This chain, located in northwest African Variscan-Alleghanian orogen, is subdivided into different segments (Fig. 1). In central Morocco, the Marrakech High Atlas (MHA) represents the southernmost segment of the Moroccan Variscan belt. It is composed of Lower Palaeozoic sequences (Early Cambrian to Ordovician age), variably affected by metamorphism and deformation during the Late Carboniferous and the main structures generated can be attributed to a main episode of Namuro-Westphalian age deformation (e.g., J. Lagarde, 1985; Cornée et al., 1987, 1990; Mabkhout et al., 1988; Piqué, 1994). Their exhumation is conditioned by late Variscan and Atlasic (Alpine) episodes (Schaer, 1964; Proust et al., 1977; Cornée et al., 1987; Dias et al., 2011; Loudaoued et al., 2023).

Significant granitic igneous activity, mainly calc-alkaline, occurred in the Moroccan Variscides between the Westphalian and Early Permian. This magmatism shows differences between the Western Moroccan Meseta with peraluminous granites and the Eastern Moroccan Meseta with potassic to shoshonitiic and calc-alkaline granitoids (e.g., Gasquet et al., 1996; El Hadi et al., 2006). The calc-alkaline nature of both the granitoids and a late-orogenic magmatism associated with the presence of amphibole-bearing rocks (diorite-tonalite-andesite), have led several workers to suggest an orogenic context, such as an active subduction zone and/or partial melting of a metasomatised upper mantle (e.g., Gasquet et al., 1996; El Hadi et al., 2003).

The main Variscan deformation in the Western Meseta took place in Westphalian-Stephanian times (320 to 290 Ma), later than in the Eastern Meseta (e.g., Mrini et al., 1992; El Hadi et al., 2006; Zouicha et al., 2022). Whole-rock radiometric ages available for the Variscan granites in the Western Meseta
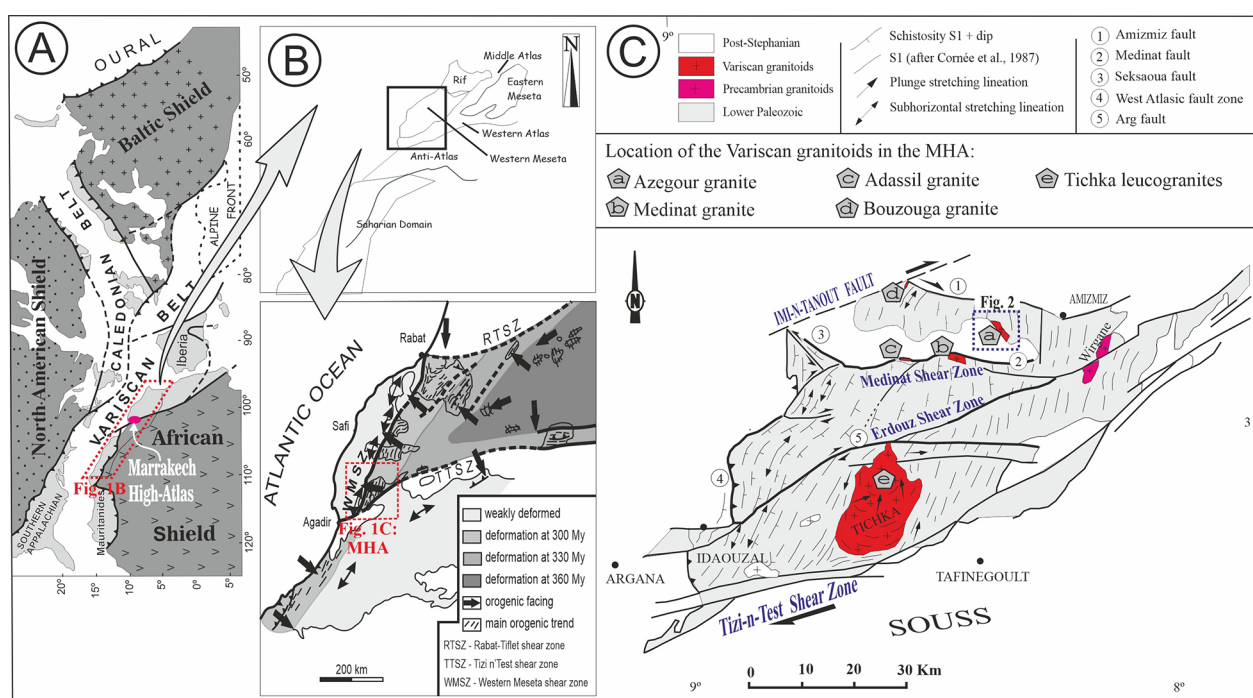
Fig. 1. A – Location of the Marrakech High Atlas (MHA) within the context of the Alleghanian-Variscan Orogeny (Ribeiro et al., 1979); **B –** Location within the northern Moroccan Variscan chain; **C –** Simplified geological map of the MHA (adapted from Cornée et al., 1987).

(Fig. 1) range between 330 and 260 Ma (e.g., Mrini et al., 1992; Gasquet et al., 1996; Essaifi et al., 2003; Marcoux et al., 2019; Chopin et al. 2023).

The aim of the present paper is to outline petrographic aspects, whole-rock geochemistry, Rb-Sr whole-rock age and Sr-Nd isotopic data of the Azegour granitoid in an attempt to contribute to the discussion about the petrogenesis of A-type granites in Variscan terrains and their tectonic setting with regard to the first main Variscan deformational event D_1.

2. Geological setting

The Marrakech High Atlas (MHA) (Fig. 1) corresponds to the southernmost fragment of the Western Meseta; it was deeply affected by Variscan orogeny during the major Westphalian-Namurian deformational event (e.g., Cornée et al., 1987, 1990; Ait Ayad et al., 2000; Berrada et al., 2011; Ibouh et al., 2011). Detailed structural mapping of the MHA has shown that the Variscan deformation is related to several crustal-scale shear zones: the coeval ENE-WSW dextral Amizmiz and Tizi-n'Test shear zones and the slightly younger WNW-ESE-trending sinistral Medinat shear zone (Hadani, 2009; Dias et al., 2011). The first major stage of deformation (D_1) is predominantly associated with dextral shearing;

it produced a N-S pervasive axial planar cleavage (S_1). The regional schistosity (S_1) passes towards the southeast at a metamorphic foliation in the vicinity of the Tichka granite (e.g., Cornée et al., 1987, 1990). At the end of this deformation phase, or relatively later, occurred the emplacement of a series of intrusions (e.g., Tichka, Adassil, Medinat and Azegour). These areas of crustal fractures are spatially favourable to the emplacement establishment of magmatic bodies. Their ascent was facilitated by the existence of NNE-SSW trending crustal anisotropies, subparallel to the Western Mesetean Shear zone (WMSZ).

In the Azegour region (Fig. 2), an intrusive body crops out over a surface area of approximately 5 x 0.8 km. Along its north-easterly edge, the massif defines discordant relationships with the metasedimentary and metavolcanic rocks, apart from the south-westerly contact which is covered by Meso-Cenozoic deposits (Fig. 2). The metasedimentary rocks are located outside the influence of contact metamorphism, containing chlorite and white micas as the main index minerals, suggesting that regional metamorphism did not exceed epizonal and/or anchizonal conditions. The Mo-W-Cu mineralisations are located within the metamorphic aureole surrounding the Azegour intrusion, and occur as irregular mineralised bodies extending in a N-S structural trending (e.g., Ait Ayad et al., 2000; Berrada et al., 2011; Ibouh et al., 2011).
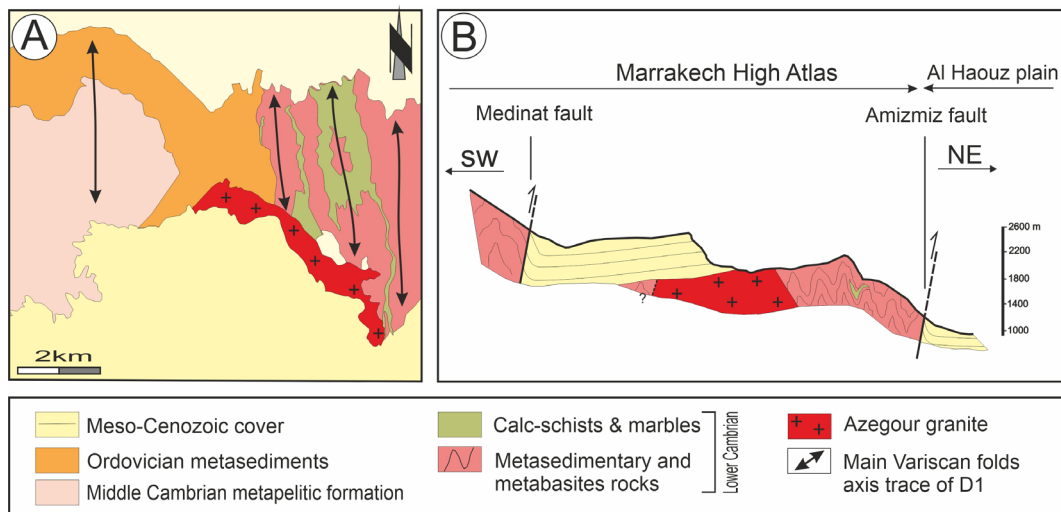
Fig. 2. A – Geological sketch map of the Azegour region showing major formations (Geological map of Amizmiz 1:100,000; SGM, 1996); **B –**Simplified geological cross-section (NE-SW) of the Azegour region (adapted from Permingeat, 1957; see location in Figure 1).

3. Analytical methods

Four representative samples from the Azegour granite, including six samples from neighbouring intrusions outcropping in the northern part of the MHA, were analysed for major and trace elements by ICP-AES (inductively coupled plasma atomic emission spectrometry) and ICP-MS (inductively coupled plasma mass spectrometry) at the Activation Laboratories Ltd (Canada). The detection limit is 0.01 per cent for all major elements and loss on ignition, except for Ti and Mn for which this limit is 0.001 per cent. For all elements, the analytical error is less than 4 per cent; results are shown in Table 1 (see Supplement).

Rb-Sr and Sm-Nd isotopic analyses of granitic samples studied were conducted at the Laboratory of Isotopic Geology of the University of Aveiro. A chemical preparation was performed following previously established analytical procedures. The samples were analysed in a solid source thermal ionization mass spectrometer, VG SECTOR 54, equipped with six moveable collectors and a fixed central. The reference used in Sr analysis was the international standard NBS 987, obtaining the value of 0.710263(10) for a grade of 95 per cent confidence in four measurements. Data were normalised to the value of $^{86}Sr/^{88}Sr = 0.1194$ (Dickin, 1997).

$^{143}Nd/^{144}Nd$ data in samples were corrected according to the law of exponential fractionation for $^{146}Nd/^{144}Nd = 0.7219$ values and normalised for ^{146}Nd La Jolla standard (Lugmair & Carlson, 1978). The Jndi-1 ($^{143}Nd/^{144}Nd = 0.5121157$, Tana-

ka et al., 2000) standard was also analysed with $^{143}Nd/^{144}Nd = 0.512114$ (2), for a confidence level of 95 per cent in 27 measurements. The values of concentrations of Rb, Sr, Sm and Nd, used for calculating ratios $^{87}Rb/^{86}Sr$ and $^{147}Sm/^{144}Nd$, were determined by ICP-MS at Activation Laboratories. For the calculation of isochrones, the software program Isoplot version 3.00 (Ludwig, 2003) was used, which calculates the regression line based on the least squares method (York, 1969). The decay constant used for ^{87}Rb was 1.42×10^{-11} year^{-1} (Steiger & Jäger, 1977). The maximum numbers of errors admitted for the $^{87}Rb/^{86}Sr$ ratio are 2 per cent.

4. Results

4.1. Petrography characteristics of the Azegour intrusion

The four sampled rocks from the Azegour granite show strong similarities between them, which points to a great homogeneity on the scale of the massif. The dominant facies exhibit a pink colour, a medium-grained phaneritic texture (Fig. 3A, B), and a mineralogical composition of quartz, potassium feldspar (microcline), plagioclase (oligoclase-albite), biotite, apatite, sphene, zircon, monazite and opaque (Fig. 3C–F).

The other samples correspond to microgranitic facies, also pink in colour, which appear in the form of centimetre-sized veins in continuity with
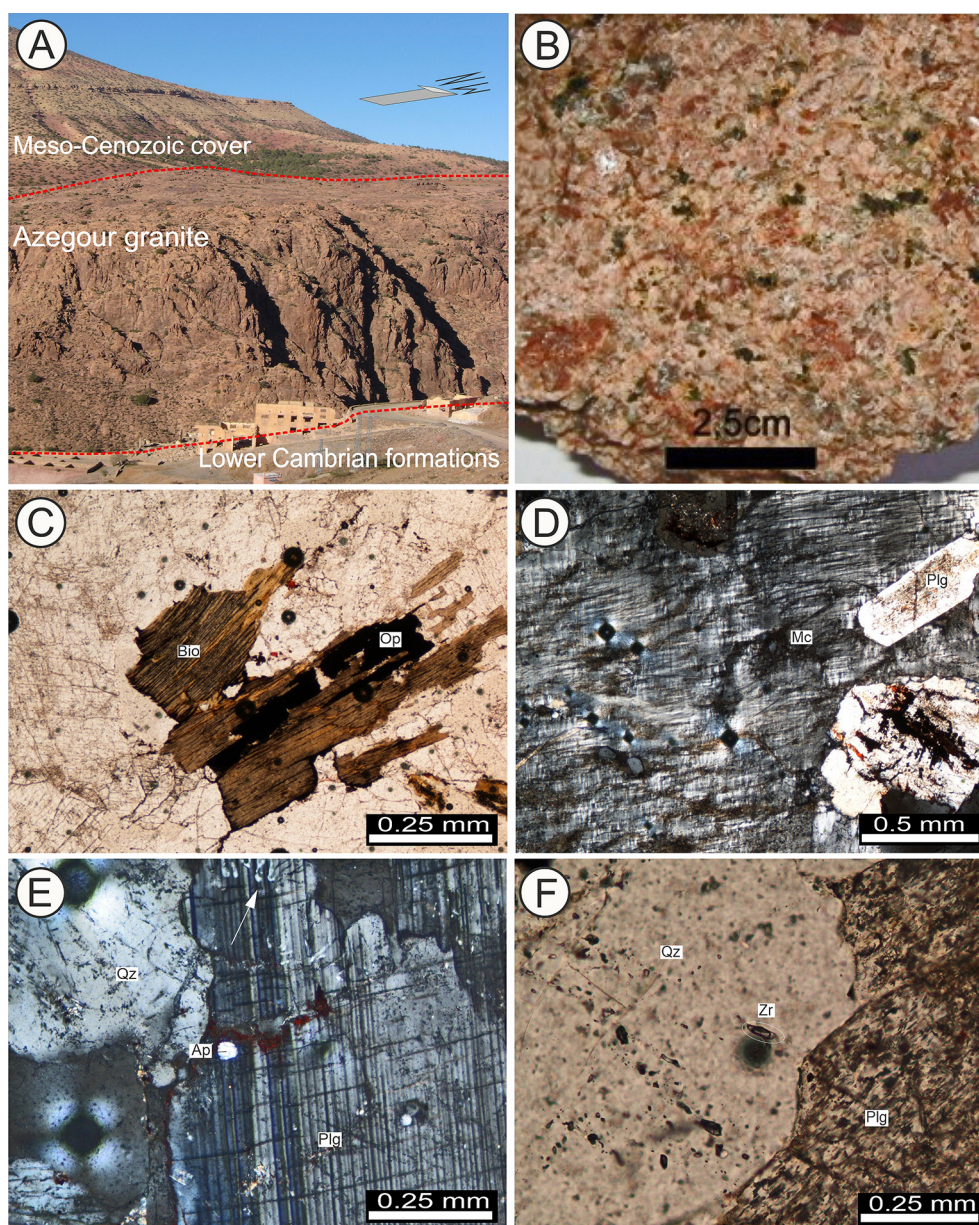
Fig. 3. Field photographs and microphotographs representative of principal facies of the Azegour granite. **A –** Panoramic view of the Azegour granite, which intrudes Lower Cambrian metasedimentary and metavolcanosedimentary rocks. Meso-Cenozoic formations overlie the south-westerly contact of the granite; **B –** Photograph of a hand specimen of the rosy-pink- coloured, medium-grained granite composed mostly of quartz, potassium feldspar (microcline), plagioclase (oligoclase-albite) and biotite; **C –** Biotite in association with opaques in the Azegour granite (plane-polarised light); **D –** Microcline-microperthite megacrystal with inclusion of a small plagioclase crystal (cross-polarised light); **E –** Plagioclase crystal with polysynthetic albite twins in contact with quartz (cross-polarised light); **F –** Zircon inclusions in quartz; intergrowth phenomena of vermicular quartz in plagioclase (myrmekite PPL). Abbreviations in microphotographs: Bio – biotite, Op – opaques, Qz – quartz, Plg – plagioclase, Mc – microcline, Ap – apatite, Bio – biotite.

the main facies. They have phaneritic texture and are fine grained. Their mineralogical composition is identical to the main facies. The scarcity of biotite is one of the most relevant characteristics of this granitoid (Permingeat, 1957).

4.2. Structural aspects

A detailed structural analysis in the Azegour region shows that the first major deformational event (D_1) produced a set of very penetrative structures,
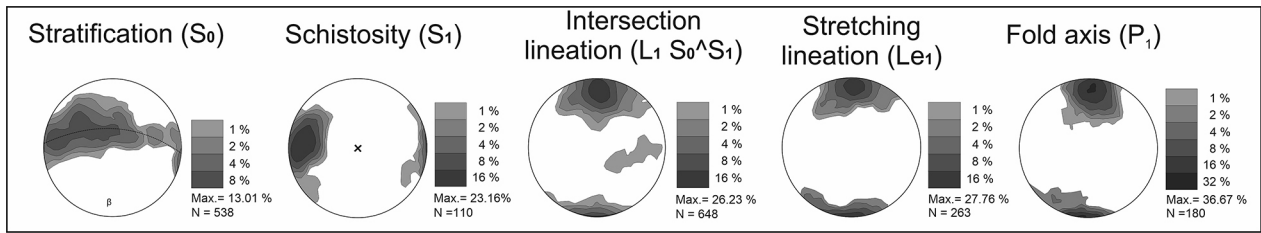
Fig. 4. Synthetic equal-area lower hemisphere stereograms of the structural elements measured in outcrops of the north-easterly metamorphic host rocks of the Azegour massif. Stereograms plotted using GEOrient 9.4 software (Holcombe, 1994).

and generated slightly N-S folds facing folds to the west with an axial planar schistosity (S_1) and a sub-horizontal stretching lineation (Fig. 4). The stereographic projection of stratification (S_0) data allows to conclude that the attitude of the fold axis displayed a weak inclination to the south or SSW quadrant. The behaviour of cleavage/schistosity (S_1) shows a general N to NNE-WSW trend and a steep dip towards the east. The distribution of the stretching lineation, the intersection lineation and the folding axis show, in general, a sub-horizontal to weak inclination trending towards the north. In addition, the stretching lineation (Le_1), materialised by stretching quartz and micas, have subparallel trends to the b-kinematic axis of N-S trending folds.

4.3. Whole-rock Rb-Sr isochron age dating

Four samples of the Azegour granite were analysed for Rb, Sr, and Sr isotopic compositions. The Rb-Sr isotopic compositions of the Azegour granite are listed in Table 2 (see Supplement). Rb and Sr con-

Fig. 5. Plot of Azegour granite samples on the ($^{87}Sr/^{86}Sr$) *vs*($^{87}Rb/^{86}Sr$) isochron diagram.

tents of the four granitic samples are 192–213 ppm and 12–46 ppm, respectively, with $^{87}Rb/^{86}Sr$ ratios of 12.15–45.58 ppm.

The excellent alignment of data in the $^{87}Sr/^{86}Sr$ *vs* $^{87}Rb/^{86}Sr$ isochron diagram, is consistent with the whole-rock isochron of 268 ± 9 Ma, with an initial ratio ($^{87}Sr/^{86}Sr$)i of 0.7049 [Mean Square Weighted Deviation (MSWD) = 0.15] (Fig. 5). The low value of MSWD (model 1, Isoplot) indicates a high confidence in analytical results. This leads to interpret the isochron age of 268 ± 9 Ma as a minimum age for the emplacement of the Azegour granite, confirming that the studied samples are congenetic.

The initial $^{87}Sr/^{86}Sr$ ratio of the Azegour granite is 0.7049 ± 0.0023, which indicates a provenance from primitive sources with strong juvenile contribution, which is compatible with significant participation of mafic/intermediate igneous rocks of the lower crust.

4.4. Whole-rock major and trace elements geochemistry

Four samples, all representative of the Azegour granite, were analysed for major, trace elements and rare earth elements (REE). Results are shown in Table 1 (see Supplement). In addition, the geochemical data (major, trace elements and REE) of the neighbouring Adassil, Medinat and Bouzouga granitoids, outcropping in the northern part of the MHA (unpublished data; Hadani, 2009) and those of the Tichka granitoids (major elements; Gasquet et al. 1992), have been used for the purpose of comparison in the present study (Table 1).

The Azegour granite samples have an extremely differentiated character (SiO_2 = 77.53–78.14%) (Fig. 6A). They present relatively low contents of Al_2O_3 (12.01–12.33 wt.%), FeO_t (0.72–0.81 wt.%), MnO (0–0.01 wt.%), MgO (0.04–0.13 wt.%), CaO (0.39–0.47 wt.%) and high values of Na_2O+K_2O (8.26–8.56 wt.%). All these characteristics are similar to those of A-type granites (e.g., Whalen et al., 1987; Eby, 1990).

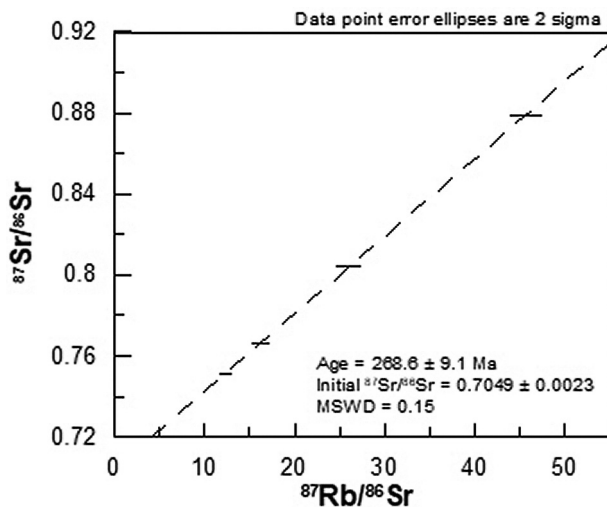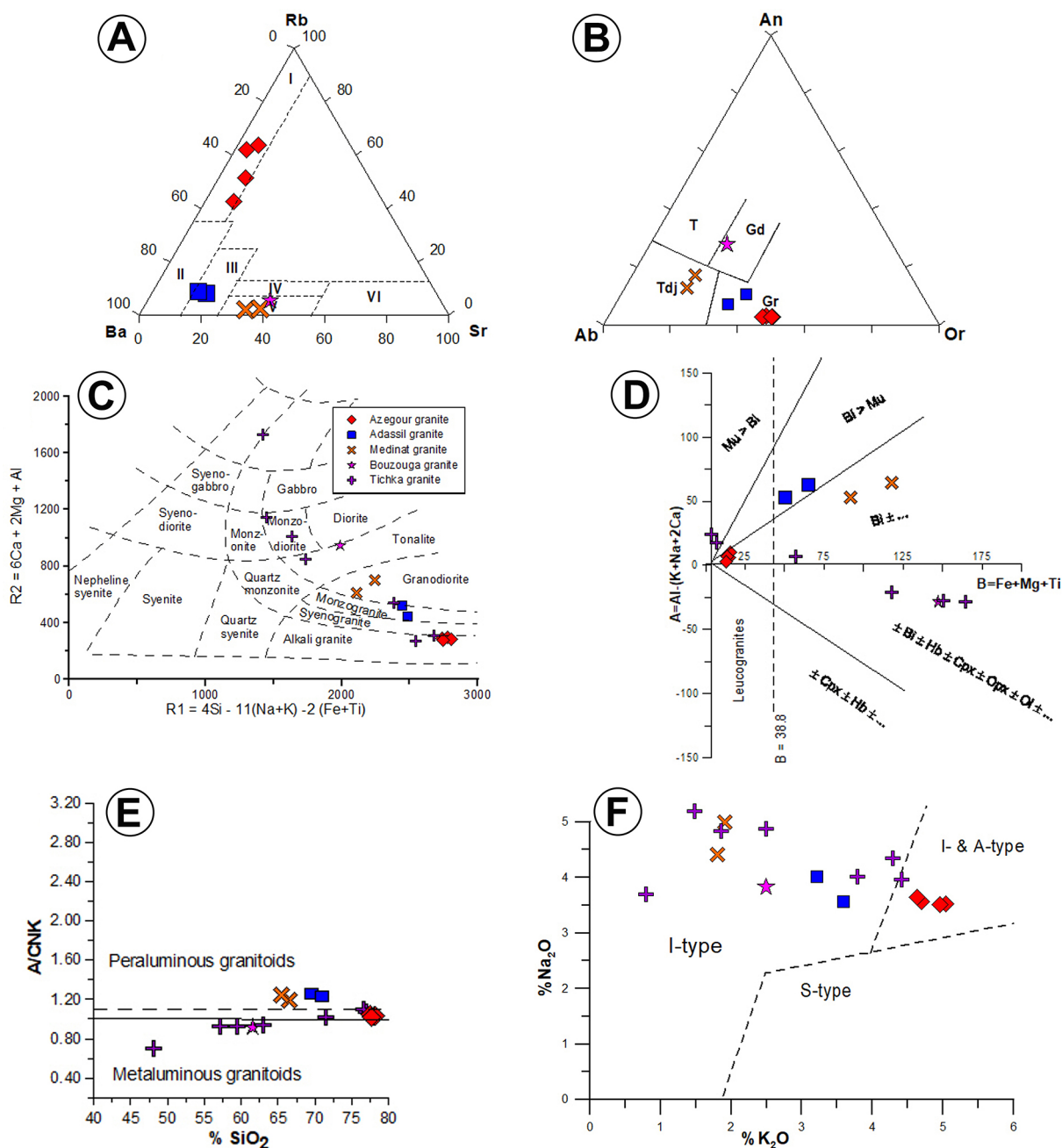**Fig. 6.** Classification of Azegour granite samples using: **A –** Rb-Ba-Sr diagram after El Bouseily & El Sokkary (1975). Abbreviations: I–very differentiated granites, II–granites, III–anomalous granites, IV–granodiorites, V–quartz-diorites, VI–diorites; **B –** Normative An-Ab-Or diagram (O'Connor, 1965; modified by Barker, 1979). Abbreviations: T – tonalites, Gd – granodiorites, Tr – trondjhemites, Gr – granites; **C –** multi-cationic R_1–R_2 diagram (De La Roche, 1980); **D –** A-B diagram after Debon & Le Fort (1983, 1988). Abbreviations: Mu – muscovite, Bi – biotite, Hb – hornblende, Cpx – clinopyroxene; **E -** A/CNK *vs* SiO_2 diagram (Clarke, 1992); **F –** Na_2O *vs* K_2O diagram (White & Chappell, 1983).

Cross, Iddings, Pirrson and Washington (CIPW) normative compositions were determined from their major oxide compositions (Table 3 in Supplement). The samples studied fall into granite field of the An-Ab-Or diagram (Barker, 1979) (Fig. 6B). When applying the multi-cationic R_1–R_2 diagram (De La Roche et al., 1980), all Azegour granite samples plot in the alkaline granite field (Fig. 6C).

In the diagram proposed by Debon & Le Fort (1983), samples from the Azegour massif plot in the leucogranite domain, with slightly positive A values (A>3.10–10.43) and very low B values (B< 13.17–15.54) (Fig. 6D). The absence of typical S-type
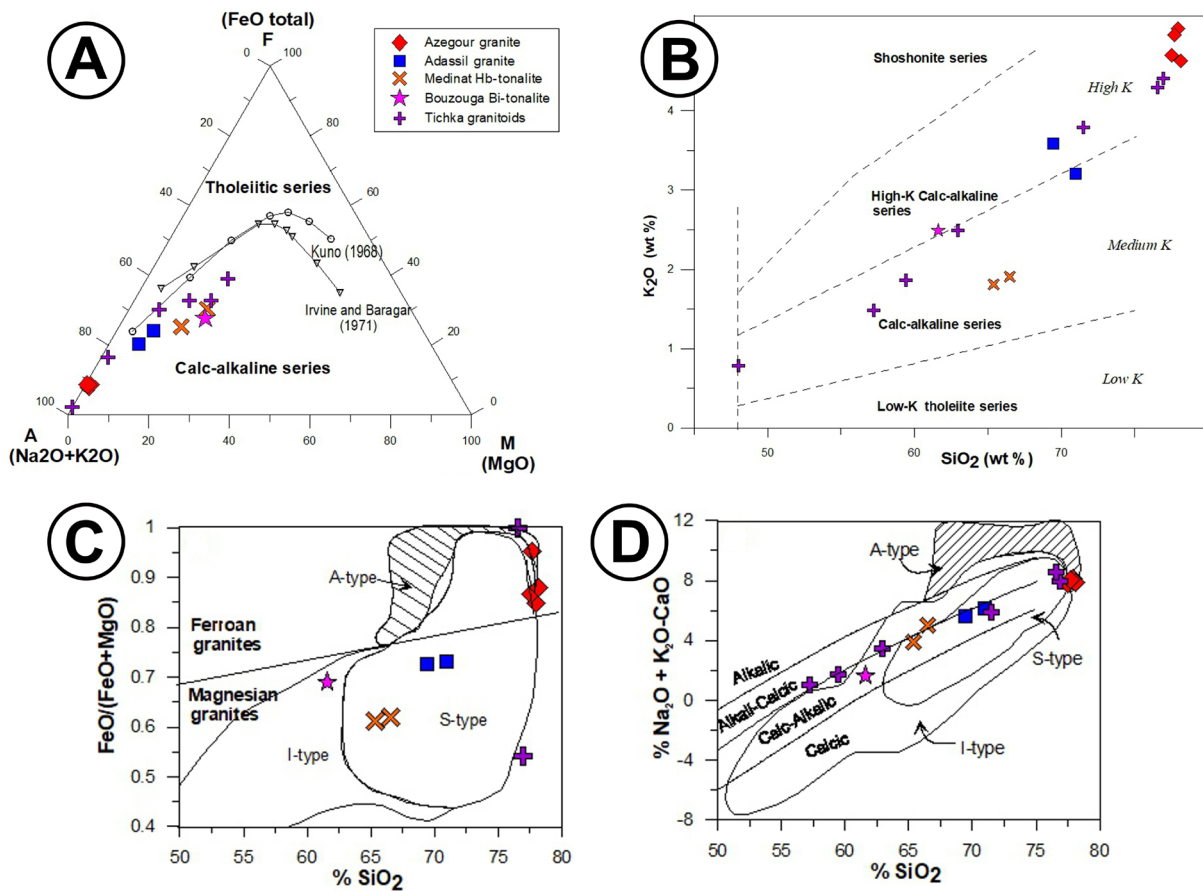
Fig. 7. Major element classification for the granite studied as well as for granitoids from the MHA. **A –** AFM diagram plot of granite samples; boundaries between tholeiitic and calc-alkaline fields are from Kuno (1968) and Irvine & Baragar (1971); **B –** K_2O vs SiO_2 diagram showing the calc-alkaline to high K-calc-alkaline affinities of granite samples (Peccerillo & Taylor, 1976); **C –** $FeOt/(FeOt+MgO)$ vs SiO_2; **D –** (Na_2O+K_2O-CaO) vs SiO_2 diagrams for granite samples (Frost et al., 2001). The shading shows the compositional spectrum of the Lachlan Fold Belt granitoids in Australia (data from Landenberger & Collins (1996) and Australian Geological Survey Organization, AGSO).

granite mineralogy (e.g., muscovite, monazite, cordierite, sillimanite and garnet) from Azegour granite samples, along with their weakly peraluminous character [A/CNK (molar $Al_2O_3/CaO+Na_2O+K_2O$) = 1,013–1,045] (Fig. 6E), suggests that supracrustal sources did not significantly contribute to their petrogenesis. These characteristics are in close concordance with an I-type or A-type affiliation for the Azegour granite (e.g., White & Chappell, 1983; Whalen, 1985; Clarke, 1992). The A-type affiliation is also confirmed in the K_2O vs Na_2O diagram (Fig. 6F).

In an AFM (Na_2O+K_2O-MgO-Fe_2O_3tot) diagram (Fig. 7A), the granitic samples display a mainly calc-alkaline signature and show a typical calc-alkaline trend. Indeed, this signature is confirmed in the K_2O vs SiO_2 diagram (Fig. 7B), showing strong K-calc-alkaline affinities of the studied

granite and the calc-alkaline affinities of the other granitoids outcropping in the MHA.

In the diagram of Frost et al. (2001), the investigated A-type granite samples plot in the calc-alkaline granitoids of a ferruginous nature field (Fig. 7C, D). According to those authors, ferriferous granitoid derives from anhydrous magmas with low oxygen fugacity, as opposed to magnesian granitoids for which an origin from the melt is postulated, with relatively high contents of water and oxygen fugacity. All samples analysed from the Azegour granite have compositional characteristics similar to A-type granitoids from the Lachlan Fold Belt region (Fig. 7C, D). The A-type affiliation for the Azegour magmas is also well expressed in the diagrams proposed by Whalen et al. (1987) (Fig. 8A–D), belonging to A1-type granites in the Nb-Y-Ce and Nb-Y-3Ga triangular diagrams (Fig. 8E, F).
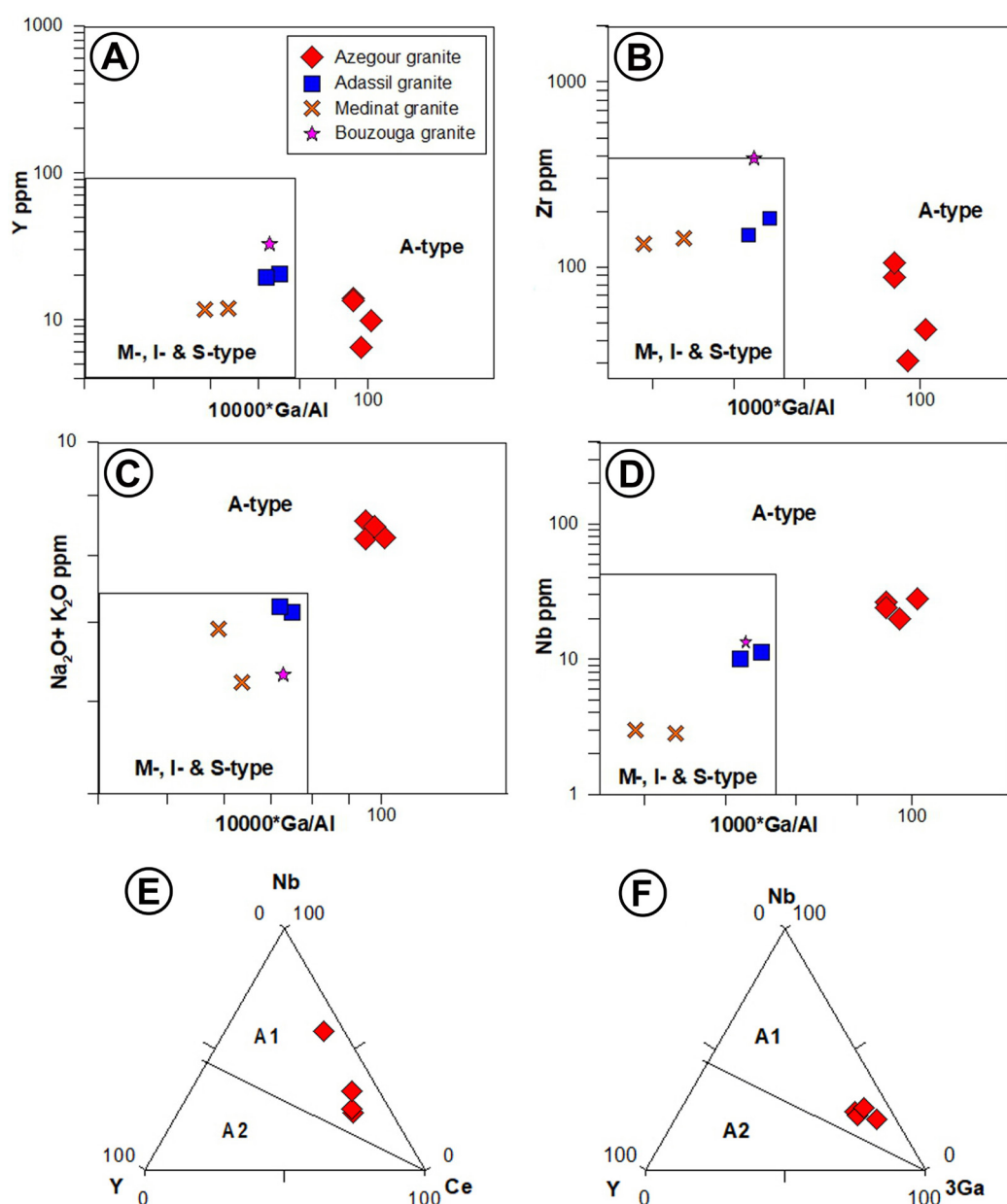
Fig. 8. Geochemical plots 1000*Ga/Al *vs* Y **(A)**, Zr **(B)**, Na$_2$O+K$_2$O,**(C),** and Nb **(D)** diagrams (Whalen et al., 1987). Abbreviations: A -, M-, S- and I-type granitoids; **E –** Nb-Y-Ce; **F –** Nb-Y-3Ga triangular diagrams applied to the Azegour granite samples (after Eby, 1992). Abbreviations: A1 – anorogenic granites, A2 – post-orogenic granites. For comparison, Tichka granitoids plot in the Whalen et al. (1987) diagrams from Gasquet et al. (1992).

4.5. Rare earth element geochemistry

The samples from the Azegour intrusion studied show weak to moderate levels of rare earth elements ($\sum$REE = 28.25–137.17 ppm), with a pronounced fractionation of LREE (La$_N$/Sm$_N$ = 7.9–13.67; Fig. 9A), consistent with enrichment in light rare earth elements (LREE) relative to heavy ones (HREE; La$_N$/Yb$_N$ = 4.81–11.61). All rock samples studied show strong negative Eu anomalies (Eu/

Eu* = 0.44–0.75). The development of negative Eu anomalies seems to have originated from fractionation of plagioclase and potassium feldspar during the evolution of the A-type magmas, which could also be explained by the high degree of depletion in Sr and Ba elements in these rocks.

In the primitive mantle-normalised, multi-element patterns for Azegour granite samples (Fig. 9B), all samples exhibit enrichment in large ion lithophile element (LILE) (Rb, Th, K) and high field
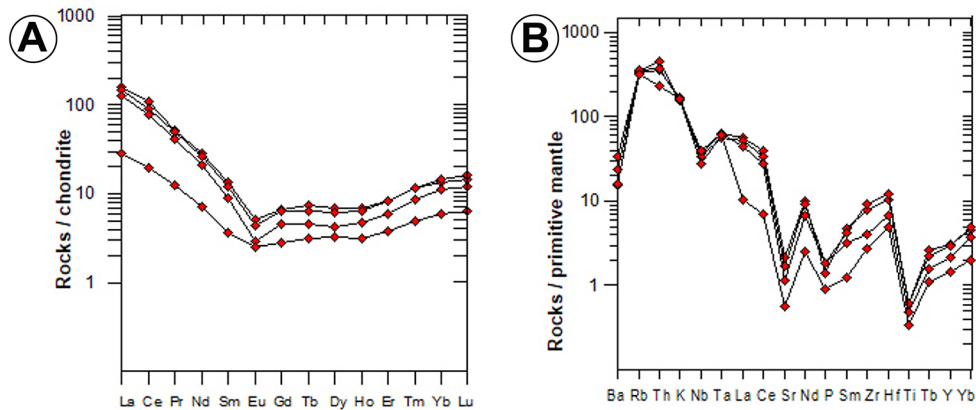
Fig. 9. A – Chondrite-normalised REE patterns (Evensen et al., 1978); **B –** Primitive mantle-normalised, multi-element patterns for the Azegour granite samples (Sun & McDonough, 1989). For comparison, the I-type magmas patterns from Brown (1991) are also shown.

strength element (HFSE) (Ta, Zr, Hf), and are considerably depleted in Ba, Sr, P, Eu, Ti and less depleted in Nb.

4.6. Whole-rock Sr-Nd isotope geochemistry

Based on available geochronological information, an age of 270 Ma was selected in order to calculate the initial $^{87}Sr/^{86}Sr$ and $^{143}Nd/^{144}Nd$ isotopic ratios of samples of the Azegour granite, as well as their values of εSr_{270} and εNd_{270} (Table 2 in Supplement, Fig. 10).

The low initial $^{87}Sr/^{86}Sr$ ratios of the samples studied ($^{87}Sr/^{86}Sr_{270}$ = 0.7040–0.7048; εSr_{270}= –1.43 to +9.32) suggest a provenance from primitive sources with a strong juvenile contribution, which is compatible with significant participation of mafic/intermediate igneous rocks of the lower crust. However, their isotopic signatures can also be attributed to interaction and/or hybridisation of basaltic liquids derived from the mantle with this type of material.

The low negative values of εNd_{270} (–0.94 to –4.85), as well as the relatively younger model ages obtained of the four samples analysed (T_{DM} = 0.11–0.83 Ga; Table 2), are compatible with both models referred to above, not allowing effective discrimination of the potential components involved in their formation. In fact, the isotopic compositions of Sr and Nd of the Azegour granite samples, when recalculated for the probable age of the intrusion, are projected in the lower right-hand quadrant of the diagram (εNd – εSr), in positions close to the mantle array and the lower crust field (Fig. 10).

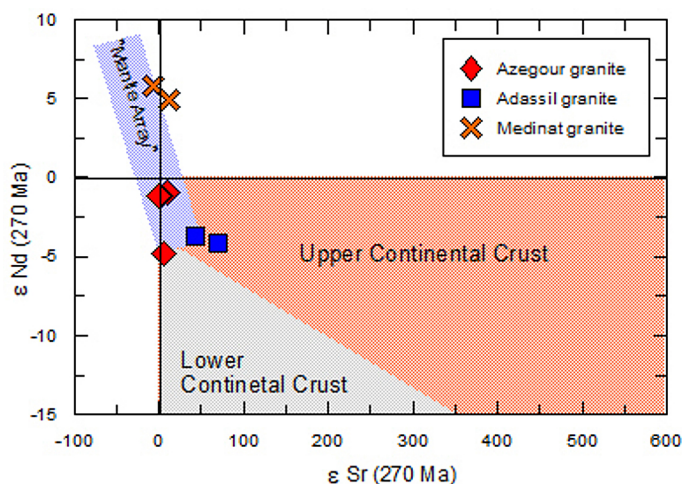**Fig. 10.** Plot of the Azegour granite samples on the $(^{143}Nd/^{144}Nd)_{270}$ *vs* $(^{87}Sr/^{86}Sr)_{270}$ diagram (DePaolo & Wasserburg, 1979; Rollinson, 1995).

5. Discussion

5.1. Significance of isochron age of the Azegour granite

The structural fieldwork data in the Azegour region allows us to understand the relationship between the granite emplacement and the deformational event in the surrounding sedimentary and volcanosedimentary host rocks. There is no geometric variation of the main schistosity (S_1) or structural lineation trajectories in the north-easterly metasedimentary rocks of the intrusion (Ait Ayad et al., 2000). The intrusion crosscuts the regional structures, imposes contact metamorphism onto the adjacent host rocks and shows no evidence of solid-state deformation. On a microscopic scale, contemporary intrusion minerals do not present any preferential orientation. All these features point to a post-kinematic (tectonic) emplacement character with regard to the main Variscan deformational event (D_1). Previous work assigned an age that ranged between 268 and 271 Ma for the emplacement of the Azegour granite with a strong mantle component (e.g., Mrini et al., 1992; AitAyad et al., 2000), which is in clear agreement with the results obtained in the present paper (268 ± 9 Ma). Although the possibility of some late isotopic re-equilibrium of the Rb-Sr system cannot be excluded, the minimum age obtained should not be too far from the age of the intrusion.

5.2. Petrogenetic characterization

The granitoid shows a calc-alkaline affinity of a ferruginous nature. The absence of a mineralogy typical of S-type granitoid, combined with its weakly peraluminous character (A/CNK = 1,013–1,045), leads to the exclusion of any significant participation of supracrustal sources in their petrogenesis. Despite the extremely differentiated character of the Azegour massif, their multi-element patterns show many similarities to those of I-type granitoids, which has led some authors to postulate that the parental liquids of I-type and A-type were both derived from partial melting under anhydrous conditions. The extraction of I-type magmas occurs at relatively early stages and causes dehydration of the source region. At a later stage, materials previously affected by partial melting processes under high temperature, in conditions of low water fugacity, contribute to the generation of A1-type magmas. The partial melting of lower crust granulitic rocks required temperatures above 850–900°C, with involvement of a mantellic component by the intrusion of basaltic magmas at the crust-mantle interface (underplating) (Clemens et al., 1986) during lithosphere extensional environments in a post-collisional tectonic setting. Thus, the hypothesis of A-type granitoids resulting from interaction processes of variable degree between mantellic mantle and crustal liquids, cannot be entirely excluded.

According to Eby (1990, 1992), A1-type granites have lower Y/Nb ratios (< 1.2) and typically originate from magmas derived from Oceanic Island Basalt (OIB) sources in intraplate or rift settings. On the other hand, A2-type granites have higher Y/Nb ratios (> 1.2) and are commonly related to post-collisional or post-orogenic settings, having primarily formed from crustal-derived melts.

5.3. Tectonic interpretation

The Azegour intrusion samples have Y/Nb ratios of 0.353–0.534 (<1.2), consistent with A-type granites and plot in the A1-type granites field of Eby's (1992) diagrams (Fig. 8). They fall within the plate granites (WPG) field (Fig. 11A, B), with one of them plotting within the syn-collision (Syn-COLG) field in the Ta *vs* Yb diagram (Fig. 11A).

In the R1–R2 tectonic discrimination diagram of Batchelor & Bowden (1985) (Fig. 11C), the Azegour intrusion samples plot in the boundary area between the anorogenic and post-orogenic fields, which does not allow to discriminate between these two tectonic settings. The samples studied have similar tectonic environments to those observed in Oceanic Island Basalts (Fig. 11D) and show therefore an affinity to an enriched mantle source, derived within intraplate settings (Fig. 12).

6. Conclusions

- Available structural data for the Azegour region allow us to understand the relationship between granite emplacement and surrounding sedimentary and vulcanosedimentary rocks. The first major event of Variscan deformation (D_1) produced a set of generally N-S trending penetrative structures and there is no geometric variation of main schistosity (S_1) or structural lineations in the vicinity of the intrusion. The emplacement of the Azegour granite seems to have been controlled by a crustal fracture oriented WNW-ESE during post-collisional time. The
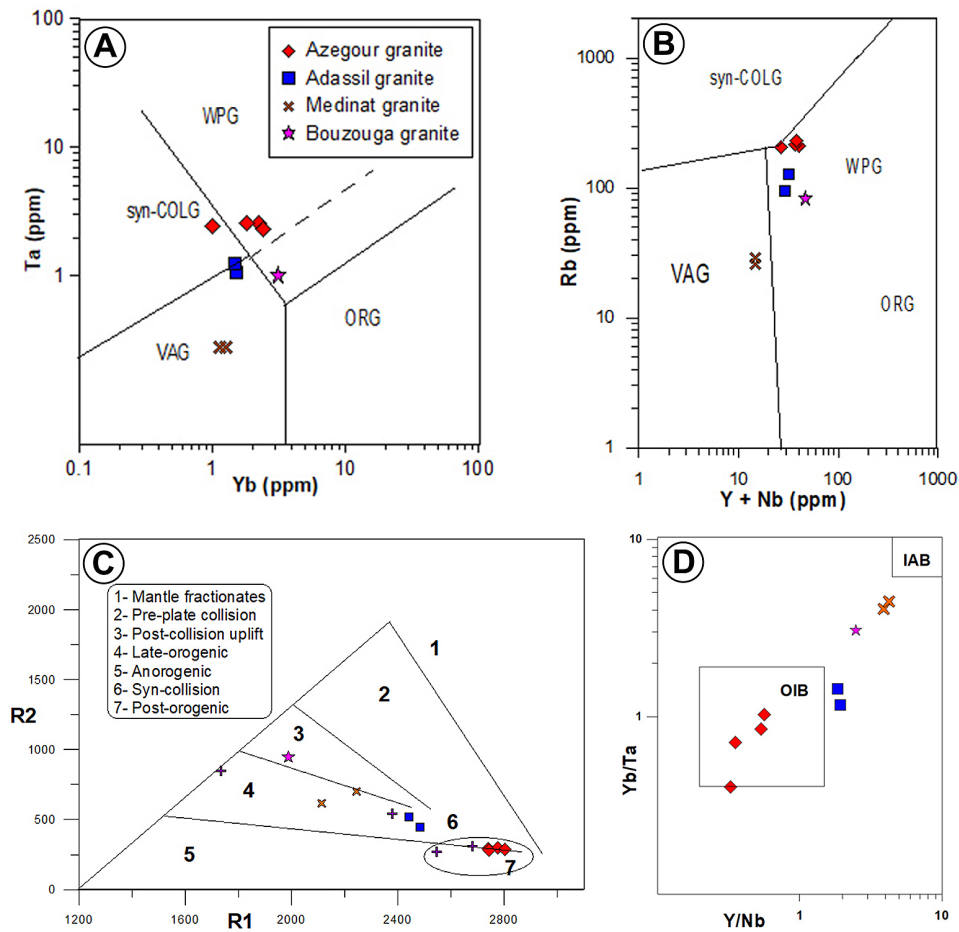
Fig. 11. Tectonic discriminant diagram plots for the Azegour granite samples and neighbouring granitoids. **A –** Ta *vs* Yb and **B –**Rb*vs* (Y+Nb) diagram (afterPearce et al. 1984; Pearce, 1996); **C –** R1-R2 tectonic discrimination diagram from Batchelor & Bowden (1985); **D –** Plot on Yb/Ta *vs* Y/Nb diagram designed to discriminate source (after Eby, 1992). The Azegour intrusion samples falls within the ocean-island basalt (OIB) field. Abbreviations: ORG – ocean ridge granites, VAG – volcanic arc granites, syn-COLG – syn-collisional granites, WPG – within-plate granites, OIB – ocean-island basalt, IAB – island arc basalts.
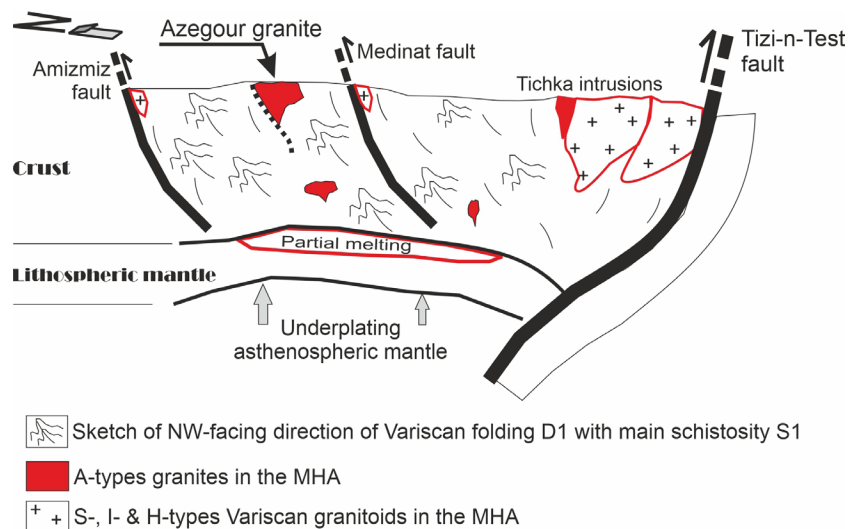
Fig. 12. Schematic cartoon showing the geodynamic model during the final stages of the Variscan orogeny, summarising the emplacement of the Azegour granite and neighbouring granitoids along crustal shear zones in the Marrakech High Atlas.

intrusion crosscuts the regional structures, imposes contact metamorphism onto the adjacent host rocks in the northern contact and shows no evidence of solid-state deformation; all these features point to a post-kinematic emplacement (post-D_1).

- The geochemical signature of the Azegour granite is compatible with an A_1-type affiliation. Given its extremely differentiated character, this granite seems to represent the most evolved stage of fractional crystallisation processes, which probably occurred at deep structural levels and involved the separation of a mineralogical association composed of plagioclase + potassium feldspar + amphibole + titanite + apatite.

- Its magmatic precursors were most likely derived from partial melts with involvement of a mantellic component by the intrusion of basaltic magmas at the crust-mantle interface (underplating), influenced by the asthenospheric mantle.

- The εSr, εNd and TD_M values of the samples studied (εSr$_{270}$ = –1.43 to +9.32, εNd$_{270}$ = –0.94 to –4.85, TD_M = 0.11 to 0.83 Ga), plot in the lower right-hand corner of the εNd*vs* – εSr diagram. There positions, close to the mantle array and the lower crust fields, suggest a provenance from primitive sources with a strong juvenile contribution, which is compatible with significant participation of mafic or intermediate igneous rocks of the lower crust at the crust-mantle interface (underplating) during lithosphere extensional environments in a post-collisional tectonic setting.

- The age obtained by the whole-rock Rb-Sr dating method for the granite samples studied dates its emplacement around 268 ± 9 Ma, illustrating the post-tectonic character of the Azegour granite. This figure also provides a reliable age estimate for the last stages of the main Variscan deformation phase (D_1) in the Marrakech High Atlas and in the Moroccan Meseta (e.g., Piqué, 1994; Hoeppffner et al., 2005; Delchini et al., 2018; Chopin et al., 2023).

- Results obtained in the present paper allow us to conclude that the Azegour granite was emplaced about 268 ± 9 myr ago, in extensional environments of post-collisional Variscan orogeny, which is in clear agreement with fieldwork data obtained.

Supplement is available on http://www.geologos.com.pl/

References

Ait Ayad, N., Ribeiro, M.L., Solá, R., Moreira M.E., Dias, R., Bouabdelli, M., Ezzouhairi, H. & Charif, A., 2000. The Azegour Granite (Morocco): geochemical mapping and geodynamic interpretation. *Communications of the Geological and Mining Institute*, Lisbon, Portugal, 87, 155–164.

Arenas, R., Martínez, S.S., Albert, R., Haissen, F., Fernández-Suárez, J., Pujol-Solà, N., Andonaegui, P., Fernández, R.D., Proenza, J.A., Garcia-Casco, A. & Gerdes, A., 2021. 100 myr cycles of oceanic lithosphere generation in peri-Gondwana: Neoproterozoic–Devonian ophiolites from the NW African–Iberian margin of Gondwana and the Variscan Orogen. *Geological Society of London Special Publications* 503, 169–184.

Barbarin, B., 1999. A review of the realtionships between granitoid types, their origin and their geodynamic environment. *Lithos* 46, 605–626.

Barker, F., 1979. Trondhjemite: definition, environment and hypotheses of origin. [In:] Barker, F. (Ed.): Trondhjemites, dacites and related rocks. *Elsevier* 1–12.

Batchelor, R.A. & Bowden, P., 1985. Petrogenetic interpretation of granitoid rock series using multicationic parameters. *Chemical Geology* 48, 43–55.

Berrada, S.H., Hajjaji, M. & Belkabir, A., 2011. Mineralogical and geochemical features of the Wollastonite deposit of Azegour, Haut-Atlas (Morocco). *Journal of African Earth Sciences* 60, 247–252.

Bonin, B., 2007. A-type granites and related rocks: Evolution of a concept, problems and prospects. *Lithos* 97, 1–29.

Brown, G.C., Thorpe, R.S. & Webb, P.C., 1984. The geochemical characteristics of granitoids in contrasting arcs and comments on magma sources. *Journal of the Geological Society of London* 141, 413–26.

Brown, M., 1991. Comparative geochemical interpretation of Permian-Triassic plutonic complexes of the Coastal Range and Altiplano (23°30′ to 26°30′S), northern Chile. *Geological Society of America* 265, 157–171.

Castro, A., 2014. The off-crust origin of granite batholiths. *Geoscience Frontiers* 5, 63–75.

Castro, A., 2021. A non-basaltic experimental cotectic array for calc-alkaline batholiths. *Lithos* 382, 105929.

Chappell, B.W. & White, A.J.R., 1974. Two contrasting granite types. *Pacific Geology* 8, 173–174.

Chappell, B.W. & White. A.J.R., 1992. I- and S-type granites in the Lachlan Fold Belt. *Transactions of the Royal Society of Edinburgh, Earth Science* 83, 1–26.

Chopin, F., Leprêtre, R., El Houicha, M., Tabaud, A.S., Schulmann, K., Míková, J., Barbarand, J. & Chebli, R., 2023. U–Pb geochronology of Variscan granitoids from the Moroccan Meseta (Northwest Africa): Tectonic implications. *Gondwana Research* 117, 274–294.

Clarke, D.B., 1992. *Granitoid rocks*. Chapman & Hall, London, 283 pp.

Clemens, J.D., Holloway, J.R. & White, A.J.R., 1986. Origin of an A-type granite: experimental constraints. *American Mineralogist* 71, 317–324.

Collerson, K.D., 1982. Geochemistry and Rb-Sr geochronology of associated Proterozoic peralkaline and subalkaline anorogenic granites from Labrador. *Contributions to Mineralogy and Petrology* 81, 126–147.

Collins, W.J., Beams, S.D., White, A.J.R. & Chappell, B.W., 1982. Nature and origin of A-type granites with particular reference to southeastern Australia. *Contributions to Mineralogy and Petrology* 80, 189–200.

Cornée, J.J., Ferrandini, J. & Bernard, S., 1987. The Western High Atlas Paleozoic, a middle Cambrian graben between two dextral strike-slip with N60ºE trend, Moroccan Variscides. *Comptes Rendus de l'Académie des Sciences* 305, 499–503.

Cornée, J.J., Muller, J. & Tayebi, M., 1990. Evidence of a late-Hercynian post-schistose overlap with suppressive character in the Western Paleozoic High Atlas (Morocco). *Comptes Rendus de l'Académie des Sciences* 305, 1521–1526.

Cui, X., Sun, M., Zhao, G., Zhang, Y. & Yao, J., 2021. Two-stage mafic-felsic magma interactions and related magma chamber processes in the arc setting: An example from the enclave-bearing calc-alkaline plutons, Chinese Altai. *Geochemistry, Geophysics, Geosystems* 22, 12.

De La Roche, H., Leterrier, J., Grandclaude, P., & Marchal, M., 1980. A classification of volcanic and plutonic rocks using R1-R2 diagram and major element analysis. Its relationships with current nomenclature. *Chemical Geology* 29, 183–210.

Debon, F. & Le Fort, P., 1983. A chemical and mineralogical classification of common plutonic rocks and associations. *Transactions of the Royal Society of Edinburgh: Earth Sciences* 73, 135–14.

Debon, F. & Le Fort, P., 1988. A cationic classification of common plutonic rocks and their magmatic classification principles, methods, applications. *Bulletin de la Société française de Minéralogie* 111, 493–510.

Delchini, S., Lahfid, A., Lacroix, B., Baudin, T., Hoepffner, C., Guerrot, C., Lach, P., Saddiqi, O. & Ramboz, C., 2018. The geological evolution of the Variscan Jebilet Massif, Morocco, inferred from new structural and geochronological analyses. *Tectonics* 37, 4470–4493.

DePaolo, D.J. & Wasserburg, G.J., 1979. Petrogenetic mixing models and Nd-Sr isotopic patterns. *Geochimica et Cosmochimica Acta* 43, 615–627.

Dias, R., Hadani, M., Leal Machado, I., Adnane, N., Hendaq, Y., Madih, K. & Matos, C., 2011. Variscan structural evolution of the western High Atlas and the Haouz plain (Morocco). *Journal of African Earth Sciences* 61, 331–342.

Dickin, A.P., 1997. *Radiogenic isotope geology*. Cambridge University Press, 452 pp.

Eby, G.N., 1990. The A-type granitoids: A review of their occurrence and chemical characteristics and speculations on their petrogenesis. *Lithos* 26, 115–134.

Eby, G.N., 1992. Chemical subdivision of the A-type granitoids: Petrogenetic and tectonic implications. *Geology* 20, 641–644.

El Bouseily, A.M. & El Sokkary, A.A., 1975. The relation between Rb, Ba and Sr in granitic rocks. *Chemical Geology* 16, 207–219.

El Hadi, H., Simancas, J.F., Tahiri, A., Lodeiro, J.F., Azor, A. & Martinez-Poyatos, D., 2006. Comparative review of the Variscan granitoids of Morocco and Iberia: proposal of a broad zonation. *Geodinamica Acta* 19(2), 103–116.

EL Hadi, H., Tahiri, A., Reddad, A., 2003. Les granites varisques post-collisionnels du Maroc Oriental: une province magmatique calc-alcaline à shoshonitique [The post-collisional Variscan granites of Eastern Morocco: a calc-alkaline to shoshonitic magmatic province]. *Comptes Rendus Géoscience* 335, 959–967.

Essaifi, A., Lagarde, J.L. & Capdevila, R., 2001. Deformation and displacement from shear zone patterns in the Variscan upper crust (Jebilet, Morocco). *Journal of African Earth Sciences* 32, 335–350.

Essaifi, A., Potrel, A., Capdevila, R. & Lagarde, J.L., 2003. Datation U-Pb: âge de mise en place du magmatisme bimodal des Jebilet centrales (chaîne Varisque, Maroc). Implications géodynamiques [U-Pb dating: age establishment of bimodal magmatism of the central Jebilet (Varisk Range, Morocco). Geodynamic implications]. *Comptes Rendus Géoscience* 335, 193–203.

Evensen, N.M., Hamilton, P.J. & O'Nions, R.K., 1978. Rare earth abundances in chondritic meteorites. *Geochimica Cosmochimica Acta* 42, 1199–1212.

Frost, B.R., Barnes, C.G., Collins, W.J., Arculus, R.J., Ellis, D.J. & Frost, C.D., 2001. A geochemical classification for granitic rocks. *Journal of Petrology* 42, 2033–2048.

Gasquet, D., Stussi, J.M. & Nachit, H., 1996. Les granites varisques du Maroc dans le cadre de l'évolution géodynamique régionale [The Variscan granites of Morocco in the context of regional geodynamic evolution]. *Bulletin de la Société Géologique de France* 167, 517–528.

Gasquet, D., Leterrier, J., Mrini, Z. & Vidal, Ph., 1992. Petrogenesis of the Hercynian Tichka Plutonic Complex (Western High Atlas, Morocco): trace element and Rb-Sr and Sm-Nd isotopic constraints. *Earth and Planetary Science Letters* 108, 29–44.

Grebennikov, A.V., 2014. A-type granites and related rocks: petrogenesis and classification. *Russian Geology and Geophysics* 55, 1353–1366.

Hadani, M., 2009. *Evolução tectono-metamórfica e magmática do sector setentrional do Alto Atlas ocidental (Marrocos)* [*Tectono-metamorphic and magmatic evolution of the northern sector of the Western High Atlas (Morocco) in the Variscan Ibero-Moroccan frame*]. Evora Univer-

sity, 267 pp. https://dspace.uevora.pt/rdpc/han-dle/10174/11112.

Hoepffner, C., Soulaimani, A. & Piquée, A., 2005. The Moroccan Hercynides. *Journal of African Earth Sciences* 43, 144–165.

Holcombe, R.J., 1994. *GEOrient – an integrated structural plotting package for MS-Windows*. Geological Society of Australia Abstract 36, 73–74.

Ibouh, H., Hibti, M., Saidi, A. & Touil, A., 2011. Cu, Mo, W metasomatic deposit at Azegour region (Western High Atlas). *Notes et Mémoires du Service Géologique du Maroc* 9, 229–233.

Irvine, T.N. & Baragar, W.R.A., 1971. A guide to the chemical classification of the common volcanic rocks. *Canadian Journal of Earth Sciences* 8, 523–548.

Kuno, H., 1968. *Differentiation of basalt magmas*. [In:] Hess, H.H. & Poldervaart, A. (Eds): Basalts: The Poldervaart treatise on rocks of basaltic composition. Interscience, New York, 623–688.

Lagarde, J., 1985. Ductile shear zones and granitic plutons emplacement contemporaneous to the post-Visean Hercynian deformation of the Moroccan Meseta. *Hercynica* 1, 29–37.

Lagarde, J.L. & Choukroune, P., 1982. Ductile shear zones and the syntectonic emplacment of granitoides: the example of the Hercynian massif of the Jebilet (Morocco). *Bulletin de la Société Géologique de France* 24, 299–307.

Landenberger, B. & Collins, W.J., 1996. Derivation of A-type granites from a dehydrated charnockitic lower crust: evidence from the Chaelundi Complex. Eastern Australia. *Journal of Petrology* 37, 145–170.

Lécuyer, C., Gasquet, D., Allemand, P., Martineau, F. & Martinez, I., 2017. Cooling history of nested plutons from the Variscan Tichka plutonic complex (Morocco). *International Journal of Earth Sciences* 106, 2855–2872.

Li, H., Watanabe, K. & Yonezu, K., 2014. Geochemistry of A-type granites in the Huangshaping polymetallic deposit (South Hunan, China): Implications for granite evolution and associated mineralization. *Journal of Asian Earth Sciences* 88, 149–167.

Liu, Z., Tan, S.C., Wang, G.C., He, X.H. & Ye, H., 2020. Granitic magmas with enriched isotopic compositions, from enriched mantle source: Implications for continental generation. *Lithos* 360, 105445.

Loiselle, M.C. & Wones, D.R., 1979. Characteristics and origin of anorogenic granites. *Geological Society of America, Abstracts with Programs* 11, 468.

Loudaoued, I., Touil, A., Aysal, N., Aissa, M., Keskin, M., Yılmaz, I. & Ouadjou, A., 2023. Volcanic rocks from Amensif-Tnirt district in the western High Atlas (Morocco): Geochemistry, magma features and new age dating. *Journal of African Earth Sciences* 205, 104975.

Ludwig, K.R., 2003. *User's manual for Isoplot 3.00*. Berkeley Geochronology Center. Special Publication 4, 70 pp.

Lugmair, G.W. & Carlson, R.W., 1978. *The Sm-Nd history of KREEP*. Proceedings of the Ninth Lunar and Planetary Science Conference, Houston, USA, 689–704.

Mabkhout, F., Bonin, B., Ait Ayad, N, Sirna, C. & Lagarde, J., 1988. The alkaline granite massifs of the Moroccan

Permian. *Comptes Rendus de l'Académie des Sciences*, Paris, 307, 163–168.

Maniar, P.D. & Piccoli, P.M., 1989. Tectonic discrimination of granitoids. *Geological Society of America Bulletin* 101, 635–643.

Marcoux, E., Breillat, N., Guerrot, C., Négrel, P., Hmima, S.B. & Selby, D., 2019. Multi-isotopic tracing (Mo, S, Pb, Re, Os) and genesis of the MoW Azegour skarn deposit (High-Atlas, Morocco). *Journal of African Earth Sciences* 155, 109–117.

Martínez Catalán, J.R., Schulmann, K. & Ghienne, J.-F., 2021. The Mid-Variscan Allochthon: Keys from correlation, partial retrodeformation and plate-tectonic reconstruction to unlock the geometry of a non-cylindrical belt. *Earth Science Reviews* 220, 103700.

Matte, P. 2001. The Variscan collage and orogeny (480–290 Ma) and the tectonic definition of the Armorica microplate: a review. *Terra Nova* 13, 122–128.

Michard, A., Soulaimani, A., Hœpffner, C., Ouanaimi, H., Baidder, L., Rjimati, E.C. & Saddiqi, O., 2010. The southwestern branch of the Variscan Belt: evidence from Morocco. *Tectonophysics* 492, 1–24.

Moyen, J.F., Laurent, O., Chelle-Michou, C., Couzinié, S., Vanderhaeghe, O., Zeh, A., Villaros, A. & Gardien, V., 2017. Collision vs. subduction-related magmatism: two contrasting ways of granite formation and implications for crustal growth. *Lithos* 277, 154–177.

Mrini, Z., Rafi, A., Duthou, J.L. & Vidal, Ph., 1992. Rb-Sr chronology of the Hercynian granitoids of Morocco: Consequences. *Bulletin de la Société géologique de France* 163, 281–291.

O'Connor, J.T., 1965. A classification for quartz-rich igneous rocks based on feldspar ratios. *US Geological Survey Professional Paper* B525, 79–84.

Pearce, J., 1996. Sources and setting of granitic rocks. *Episodes* 19, 120–125.

Pearce, J.A., Harris, N.G.W. & Tindle, A.G., 1984. Trace element discrimination diagrams for the tectonic interpretation of granitic rocks. *Journal of Petrology* 25, 956–83.

Peccerillo, A. & Taylor, S.R., 1976. Geochemistry of Eocene calc-alkaline volcanic rocks from the Kastamonu area, northern Turkey. *Contributions to Mineralogy and Petrology* 58, 63–81.

Permingeat, F., 1957. *The molybdenum, tungsten and copper deposit of Azegour (Western High Atlas), petrographic and metallogenic studies*. Notes et Mémoires du Service Géologique du Maroc, 141 pp.

Piqué, A., 1994. *Geology of Morocco, regional domains and their structural evolution*. Imprimerie El Maarif, El Jadida, 278 pp.

Pitcher, W.S., 1983. *Granite type and tectonic environment*. [In:] K. Hsu (Ed.): Mountain building processes. Academic Press, London, 1940.

Proust, F., Petit, J.P. & Tapponnier, P., 1977. The Tizi-n'Test accident and the role of strike slip in the Western High Atlas tectonics. *Bulletin de la Société Géologique de France* 7, 541–551.

Ribeiro, A., Antunes, M.T., Ferreira, M.P., Rocha, R.B., Soares, A.F., Zbyszewski, G., Moitinho De Almeida, F., Carvalho, D. & Monteiro, J.H., 1979. *Introduction to*

the general geology of Portugal. Serviços Geológicos de Portugal. Lisboa, 114 pp.

Rollinson, H., 1995. *Using geochemical data: evaluation, presentation, interpretation*. Longman Scientific & Technical, London, 352 pp.

Schaer, J.P., 1964. Cambrian volcanism in the Western High Atlas Mountains. *Comptes Rendus de l'Académie des Sciences* 258, 2114–2117.

SGM, 1996. *Notes and Memoirs Nº 372, Geological Services, Morocco. Geological map of Amizmiz at a scale of 1:100 000. Feuille NH-29-XXII-2*.

Steiger, R.H. & Jäger, E., 1977. Subcomission on geochronology: convention on the use of decay constants in geo- and cosmochronology. *Earth and Planetary Science Letters* 36, 359–362.

Sun, S.S. & McDonough, W.F., 1989. *Chemical and isotopic systematics of oceanic basalts: Implications for mantle composition and processes*. [In:] Saunders, A.D. & Norry, M.J., (Ed.): Magmatism in the ocean basins. Geological Society, London, Special Publications 42, 313–345.

Tanaka, T., Togashi, S., Kamioka, H., Amakawa, H., Kagami, H. & Hamamoto, T., 2000. Jndi-1: a neodymium isotopic reference in consistency with lajolla neodymium. *Chemical Geology* 168, 279–281.

Vigneresse, J.L., 1995. Control of granite emplacement by regional deformation. *Tectonophysics* 249, 173–186.

Vonopartis, L.C., Kinnaird, J.A., Nex, P.A. & Robb, L.J., 2021. African A-Type granites: A geochemical review on metallogenic potential. *Lithos* 396, 106229.

Whalen, J.B., 1985. Geochemistry of an island-arc plutonic suite: the Uasilau-Yau Yau intrusive complex, New Britain, PNG. *Journal of Petrology* 26, 319–327.

Whalen, J.B., 1986. *Geochemistry of the mafic and volcanic components of the Topsails igneous suite, western Newfoundland*. Current Research, Part B. Geological Survey of Canada 86–1B, 121–130.

Whalen, J.B. & Currie, K.L., 1984. The Topsails igneous terrane, W. Newfoundland: evidence of magma mixing. *Contributions to Mineralogy and Petrology* 87, 319–27.

Whalen, J.B., Currie, K.L. & Chappell, B.E., 1987. A-type granites: geochemical characteristics, discrimination and petrogenesis. *Contributions to Mineralogy and Petrology* 95, 407–419.

White, A.J.R. & Chappell, B.W., 1983. Granitoid types and their distribution in the Lachlan Fold Belt, southeastern Australia. *Geological Society of America Memoirs* 159, 21–34.

Zouicha, A., Saber, H., Attari, A.E., Zouheir, T. & Ronchi, A., 2022. Late Hercynian tectonic evolution of the Jebilet Massif (Western Meseta, Morocco) based on tectono-sedimentary analyses of related Permian continental deposits. *Journal of Iberian Geology* 48, 377–403.